**2-D profiles of the flame front in turbulent premixed flames using laser induced fluorescence and laser Mie scattering**

Wong, R.; Sautet, J. C.; Snelling, David; Smallwood, Gregory; Gulder, O. L.

# 2-D PROFILES OF THE FLAME FRONT IN TURBULENT PREMIXED FLAMES USING LASER INDUCED FLUORESCENCE AND LASER MIE SCATTERING

R. Wong, J.C. Sautet, D.R. Snelling, G.J. Smallwood, Ö.L. Gülder
National Research Council of Canada, Combustion and Fluids Engineering
Building M-9, Montreal Road, Ottawa, Ont. K1A 0R6

## Introduction

The development of laser based two-dimensional (2-D) imaging techniques has proven to be an invaluable, diagnostic tool in investigating the effects of turbulence on the flame front geometry [1]. In these applications, a cross-sectional view of the 3-D flame front is obtained from the optical interaction of the laser sheet with the intersecting flame front surface. Two such techniques are Laser Induced Fluorescence (LIF) and Laser Mie Scattering (LMS). These techniques exploit different properties of the flame front. In the application of OH LIF, the flame front is the boundary marked by the large OH radical concentration gradient existing between the burnt and unburnt gases. In the application of LMS, the density gradient of the seeding agent across the flame front is used as the marker. For turbulent combustion, the resulting 2-D flame front image is a wrinkled contour outline. Recent investigations in turbulent premixed flames have shown that the geometry of the contour can be characterized using fractal analysis [2-6]. Gouldin [7] was the first to use the results of fractal analysis to predict the turbulent flame speed. The principal goal of this research program is to investigate the range of conditions in turbulent premixed flames for which a fractal description of the flame front surface is valid. This involves looking at the length scale behaviour of individual flame front contours and requires an experimental system capable of resolving to the smallest scale of wrinkling. The aim of this paper is to describe our experimental system which was developed to image the flame front in turbulent premixed propane/air flames using both LIF and LMS techniques. The relative merits of these techniques are discussed and the experimental procedures used to acquire the images are detailed.

## Experimental Apparatus

### Optical System

The OH LIF and LMS imaging systems are identical except for the light detectors used. A schematic of the optical system is shown in Fig. 1. Both systems employ a tunable wavelength XeCl excimer laser (Lambda Physiks EMG 150T MSC) that provides 140 mJ of pulse energy of about 15 ns duration. The peak laser power is about an order of magnitude greater than conventional Nd: YAG pumped dye laser systems resulting in an improved signal to noise ratio (SNR) of the optical signal. This is especially important in laser based imaging applications in which the output beam is often expanded to several times its size for an increased field of view. Normally, the laser is run at a 5 Hz repetition rate and in the narrowline mode of operation at about 308 nm. In spectral regions of high locking efficiency[1], the laser linewidth is about 2.5 pm. Fig. 2 shows the experimentally determined locking efficiency curve for the XeCl excimer gas and the overlapping OH transitions between the $A^2\Sigma^+(v=0) \leftarrow X^2\Pi(v=0)$ electronic states. Note that there are only a few OH transitions lying within the narrowline tuning range of the XeCl laser. Because of its limited spectral tuning range, XeCl tunable excimer lasers are not particulary well-suited for quantitative applications (ie. temperature measurements), in which several transitions are required [8]. Its use, therefore, has mainly been limited to qualitative, species imaging applications as is the case here. For OH LIF imaging the laser wavelength is tuned to the $Q_1(3)$ transition. For LMS imaging, the wavelength choice is somewhat arbitrary because OH LIF signals are too weak to be detected by the CCD detector and cause interference. However, there is a slight improvement in the beam divergence in running the laser narrowline as opposed to broadband operation [9]. The wavelength was therefore set to a narrowline position, at 307.9 nm. The sheet optics is a two lens system consisting of a 50 mm diameter, -102 mm focal length cylindrical lense (for vertical plane expansion) and a 75 mm diameter, 1000 mm focal length spherical lense (for horizontal plane focussing). The resulting dimensions of the sheet are approximately

[1] The locking efficiency is defined as the ratio of the energy in the narrowline part to the total pulse energy.

17 cm high and 100 $\mu$m (full width half maximum (FWHM)) at the burner centerline. Measurements of the beam width taken along the laser axial direction indicate that the beam width increases to 150 $\mu$m at a distance of 20 mm (in both directions) from the burner centerline. A 105 mm focal length, f/4.5 Nikon UV-Nikkor lens is used to collect and image the light signal (fluorescence or Mie scatter) onto the optical detector. The lens is attached to an interference filter centered at 308 nm and having a spectral bandpass of 60 nm (FWHM). For OH LIF imaging, an intensified charge-coupled device (ICCD) detector (Princeton Instruments) is used (578x384 format, 23 $\mu$m square pixel). For LMS imaging, a large format CCD (Princeton Instruments) is used (1242x1152 format, 23 $\mu$m square pixel). Both detectors are cooled to −30°C. The exposure time of the ICCD and CCD detectors are controlled, respectively, by a variable width, high voltage (HV) pulse to the intensifier and a mechanical shutter. The spatial resolution of both detectors is measured using a standard resolution test target. The large format CCD and ICCD detectors have measured spatial resolutions of 1 and 1.5 pixels, respectively. At high magnifications (image size to object size), the spatial resolution of the measurement is limited by the thickness of the laser beam. For our laser, this value is 150 $\mu$m and should be sufficiently small to resolve the finest scales of wrinkling in our flame. The functions of the detector controller are to readout the CCD, to digitize the signal and to transfer the data to the laboratory PC for processing. The ICCD and CCD detectors are digitized to 14-bit (16383) and 16-bit (65535), respectively. A custom built timing circuit is used to synchronize the firing of the laser to the readout scan of the ICCD (or CCD) detector and to supply the high voltage pulse signal to the ICCD intensifier.

### Premixed Burner and Seeding System

The premixed burner is generated by a bunsen type piloted burner of 25 mm inner diameter. Air and propane are premixed in a pipe section packed with glass beads before entering axially into the bottom of the burner. The gas flows are monitored with calibrated rotameters. Seed particles are introduced into the air/propane premixture at a point just before the entrance to the bottom of the burner. Two types of seed particles are tested for LMS imaging of the flame front. One seed is the standard aspherical aluminum oxide lens polishing agent in which most of the particles have a characteristic dimension of about 2 $\mu$m. The second seed is a plasma-alumina hollow sphere with a mean particle diameter of 6 $\mu$m. The burner shape consists of a vertical entrance section with a flat perforated baffle disk to disperse and deflect the flow. This is followed by an expansion section, a settling chamber, a contraction nozzle and finally, a straight exit section. The settling chamber contains 5 evenly spaced mesh screens to evenly distribute the flow. The burner can accommodate different nozzle diameters to vary the L/d flow parameter. Turbulence is generated using a grid placed 3 nozzle diameters upstream of the exit. The grid consists of evenly spaced holes of specific dimensions. Grids of different hole diameters and spacing are used to generate different turbulent flow characteristics. The turbulent flow characteristics are quantified for all grids studied using an Aerometrics Phase Doppler Particle Analyzer (PDPA) system but these results are not reported here. A propane pilot flame is used to prevent flame extinction and to ensure the flame remains attached to the burner exit. Finally, the burner is mounted on a fine positioning, multi-axis (x,y,z) translation table.

## Results

### OH LIF imaging

The flame front images acquired using OH LIF exhibit excellent signal to noise characteristics. The main source of noise in these images result from background flame radiation. Using an exposure time of 150 ns, the background flame radiation was suppressed to a maximum signal level of 150 counts. This is negligible compared to typical OH LIF signal levels of 5000-15000 counts. In preliminary work, OH signal levels were found to be sufficiently strong to saturate the ICCD detector. This problem was resolved by reducing the intensifer gain and/or stopping down the lens aperture. Fig. 3a and 3b show OH LIF images acquired at spatial resolutions of 350 $\mu$m and 150 $\mu$m, respectively. The flame front is marked by a large OH concentration gradient existing between the cold flow and the burnt gas region. These images also show the existence of OH in the hot burnt gas region. OH has a chemical lifetime of about 3 ms [10] in flames; assuming that velocity steamlines of 5-10 m/s are typical in our flame, an OH radical produced in the flame front would travel a distance of 15-30 mm into the hot gas region. The acquisition of OH LIF images is exceptionally fast. It takes approximately 9 minutes to acquire 100 full frame images.

### LMS imaging

The SNR of the LMS images is significantly lower than that associated with the OH LIF images. This is due to an increase in flame background radiation caused by the longer exposure time associated with a mechanical shutter. The SNR is found to improve considerably by first acquiring a background flame radiation image and then subtracting it from the unprocessed LMS image. In order to clearly visualize the flame front, it was necessary to seed the flame heavily with the aspherical aluminum oxide. An attempt was made to seed the flame with the plasma-alumina hollow spheres but we could not achieve a sufficiently high seed density to discern the flame front. The use of this seed was subsequently abandoned. Fig. 4 shows a LMS image acquired using a seed (aspherical) density of ~$10^{11}$ $m^{-3}$. At such a high seed density, there are potential problems in the measurement that need to be addressed. First, the seed may introduce a large temperature load on the flame in which case the measurement may no longer be considered nonperturbing. If the size of the aspherical aluminum oxide particles are approximated by a 2 $\mu$m diameter sphere, and using a seed density of $10^{11}$ $m^{-3}$, the temperature load is calculated to be approximately 100 K. Another problem is the influence of secondary scattered radiation on the LMS images. That is, primary scattered light may be rescattered from seed particles exterior to the plane of the laser and imaged onto the optical detector. The effect of secondary scattering is to degrade the spatial resolution of the measurement. Current investigation is underway to better quantify this effect on our LMS images. On the operational side, the aspherical aluminum oxide seed is difficult to use for a sustained period of time. It tends to agglomerate easily and sticks readily to any surface it comes in contact with. During experimental operation, the burner was dismantled and cleansed after every 30-50 image acquisitions. One potential solution to these problems is to use silicone oil as the seeding agent. With its smaller diameter, the temperature load and secondary scattering effects should be less [11].

## Summary

Images of the flame front acquired using OH LIF exhibit excellent signal to noise characteristics. The flame front is marked by a sharp OH concentration gradient existing between the burnt and unburnt gas regions and this is clearly visible in our images. Images of the flame front acquired using LMS have a higher noise level because of increased levels of flame background radiation caused by the longer exposure time associated with a mechanical shutter. To identify the flame front, a seed density of $10^{11}$ $m^{-3}$ is used in the case of aspherical aluminum oxide. At this high seed density, the temperature loading introduces a significant perturbation to the flame. The effects of secondary scattered radiation on the image spatial resolution needs to be investigated.

## Acknowledgements

We would like to thank Mr. Reg Smith for his able technical assistance on the experimental setup. Partial support for this work has been provided by EMR/PERD program.

## References

1. Sreenivasan, K.R. 1991: Fractals and multifractals in fluid turbulence. Annu. Rev. Fluid Mech. 23, 539-600
2. Gouldin, F.C., Hilton, S.M., and Lamb, T., Twenty-Second Symposium (International) on Combustion, The Combustion Institute, p. 541, 1988
3. Goix, P.J., Shepherd, L.G., Trinite, M., Combust. Sci. Technol., 63, p. 273-287, 1987
4. Mantzaras, J., Felton, P.G., Bracco, F.V., Combust. Flame 77, p. 295-310, 1989
5. Murayama, M., Takeno, T., Twenty-Second Symposium (International) on Combustion, The Combustion Institute, p. 551-559, 1988
6. Shepherd, I.G., Cheng, R.K., Talbot, L., Experiments in Fluids, 13, p. 386-392, 1992
7. Gouldin, F.C., Combust. Flame, 68, p. 249-266
8. Eckbreth, A.C., Laser Diagnostics for Combustion Temperature and Species, Abacus Press, 1988
9. Lambda Physiks EMG 150T MSC product notes
10. Barlow, R.S., Dibble, R.W., Chen, J.Y., Lucht, R.P., Combust. Flame, 82, p. 235-251, 1990
11. Chew, T.C., Britter, R.E., Bray, K.N.C., Combust. Flame, 75, p. 165-174, 1989

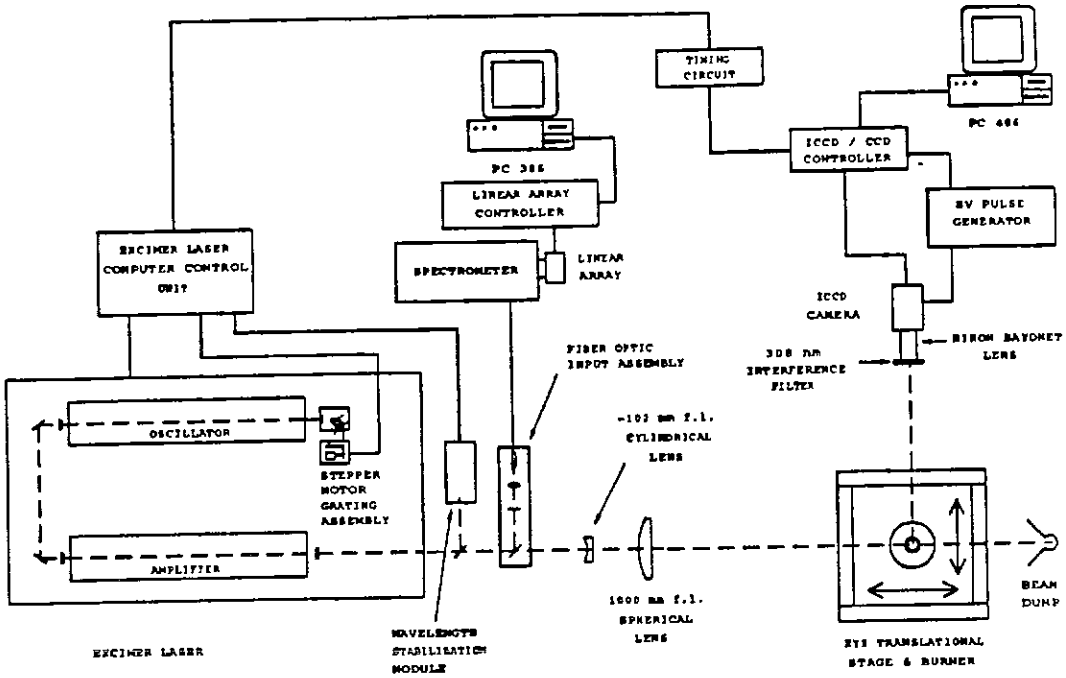


Fig. 1 Schematic of optical system

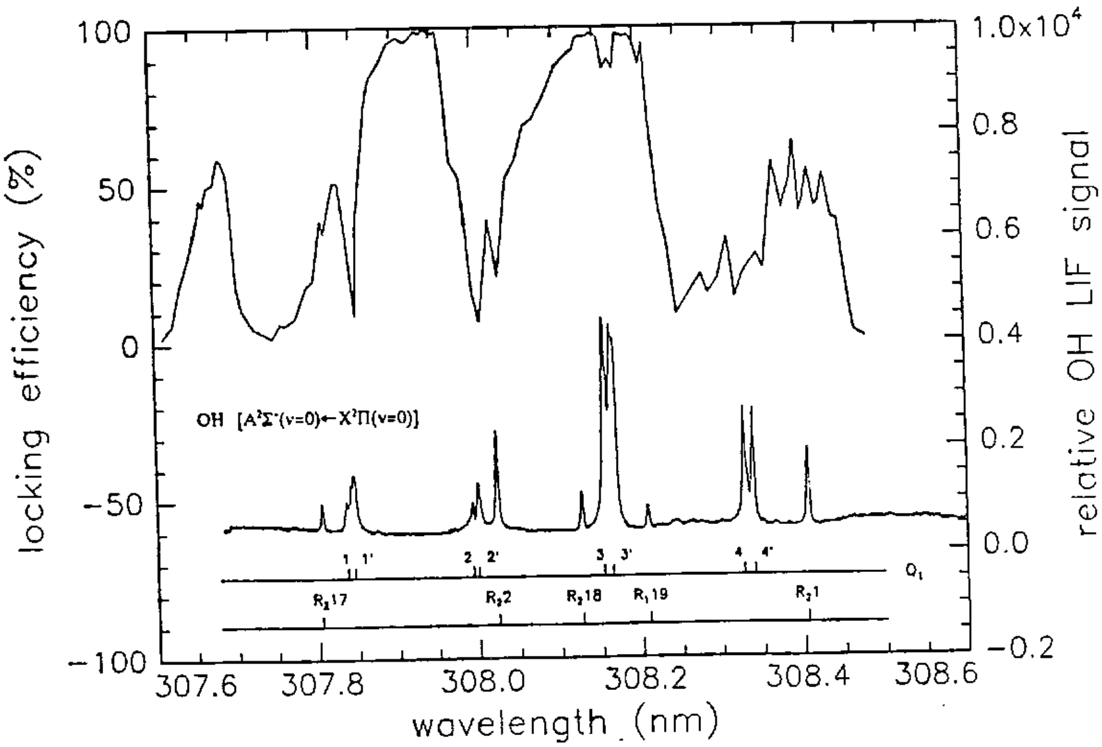


Fig. 2 Experimentally determined locking efficiency curve for the XeCl excimer laser. Also shown are the overlapping OH transitions

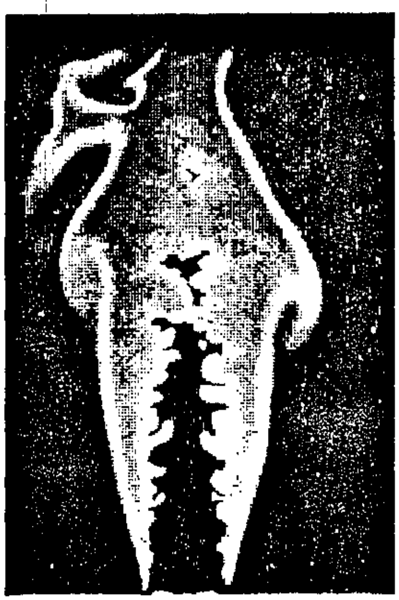

Fig. 3a

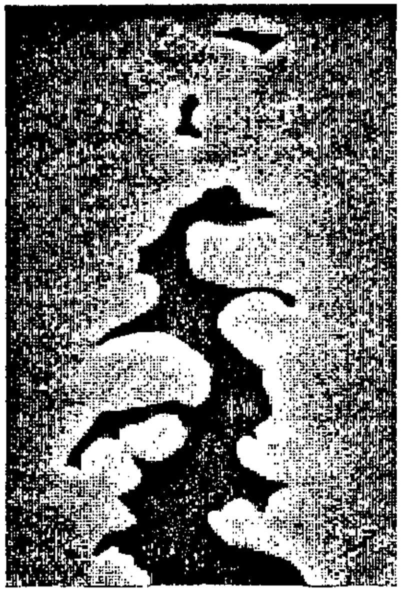

Fig. 3b

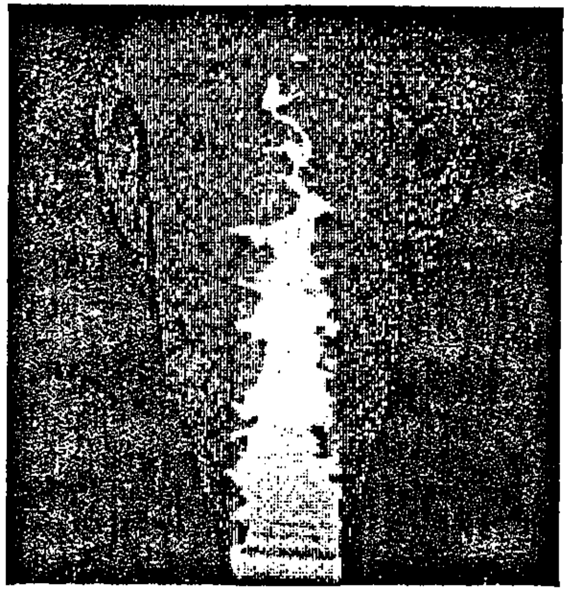

Fig. 4

Fig. 3a-b Single shot, instantaneous images of the flame front acquired using OH LIF. Fig. 3a was acquired at a magnification of 1:13.5 and Fig. 3b at 1:4.8. The spatial resolution of the measurement in the flowfield is 350 $\mu m$ in Fig. 3a, and 150 $\mu m$ in Fig. 3b.

Fig. 4 Single shot, instantaneous image of the flame front acquired using LMS and at a magnification of 1:4.5. The spatial resolution of the measurement is limited by the laser beam width and is 150 $\mu m$.

Gulder

O.L. GULDER

# The Combustion Institute
# Canadian Section

## 1993 Spring Technical Meeting

09 to 12 May 1993
Université Laval
Québec QC

UNIVERSITÉ
LAVAL